D0 Note 5332-Conf

Search for the Higgs boson in events with $H \to WW^* \to \mu + \tau_{had}$ signature with 1 fb^{-1} at D0 in Run II

The D0 Collaboration

(Dated: July 25, 2007)

A search for the Higgs boson is presented in $H \to WW^* \to \mu\tau_{had}$ decays in $p\overline{p}$ collisions at a center-of-mass energy of $\sqrt{s} = 1.96$ TeV. Final states containing hadronically decaying tau $\tau^{\pm}$ as well as $\mu + e$ events where an e is misreconstructed as τ have been considered. In order to stay orthogonal in the analysis at hand a veto on events selected by the corresponding $H \to WW^* \to e\mu$ analysis is applied. The data, corresponding to an integrated luminosity of about ~ 1000 pb^{-1}, has been collected from April 2002 to November 2005 using the Run II $D0$ detector. No significant excess above the Standard Model background has been observed, and limits on the cross section for $m_H = 120, 140, 160$ and 180 GeV have been set.

Preliminary Results for Summer 2007 Conferences

I. INTRODUCTION

In this note a search for the Higgs boson decaying into the WW^* final state with the D0 detector at the Tevatron collider at $\sqrt{s} = 1.96$ TeV at Fermilab is presented. Leptonic decay modes $H \to WW^* \to \mu + \tau_{had}^{1-prong}$ are considered, leading to final states with one muon, a jet originating from a hadronically decaying tau and missing transverse momentum. Additionally $H \to WW^* \to e + \mu$ events with the e misreconstructed as τ have been taken into account provided this events have not been selected by the $H \to WW^* \to e + \mu$ analysis. The $H \to WW^* \to \ell\ell$ decay mode provides the largest sensitivity for the Standard Model Higgs boson search at the Tevatron with a mass of $m_{\rm H} \sim 160$ GeV [1–3]. Additionally the Higgs boson masses $m_{\rm H} \sim 120, 140$ and 180 GeV have been analyzed. The present analysis taking advantage of the $\mu + \tau_{had}$ final state is complementary to the $H \to WW^* \to \ell\ell'(\ell, \ell' e = e, \mu)$ analysis presented in [4]
When combined with searches exploiting the WH and ZH associated production, this decay mode increases the sensitivity for Higgs boson searches.

II. DATA AND MC SAMPLES

The data sample used in this analysis has been collected between April 2002 and November 2005 by the D0 detector at the Fermilab Tevatron Collider. The NNLO $Z/\gamma^* \to \tau\tau$ cross section has been scaled to the data in the mass region 35 GeV$< M_{\tau\tau} <$75 GeV. Applying this normalization leads to a total luminosity $\times$ trigger efficiency of $\sim 1000\ pb^{-1}$. DATA to Monte Carlod (MC) muon correction factors have been applied to MC before normalization to $Z/\gamma^* \to \tau\tau$. The systematic uncertainties on the normalization factor include the $Z/\gamma^* \to ll$ cross section, the PDF uncertainty and the statistical uncertainty on the data/Monte Carlo normalization factor. As the MC is normalized to data, luminosity blocks marked bad by the luminosity system are retained. To maximize the sensitivity an OR of all available triggers has been applied.
Signal and Standard Model background processes have been generated with the PYTHIA 6.319 [5] Monte Carlo (MC) generator using the CTEQ6L1 parton distribution functions and subsequent use of GEANT which provides a detailed simulation of the detector geometry. MC events are then processed further with the same reconstruction software as used for data. All background processes, apart from QCD multijet production, are normalized using cross sections calculated at next-to-leading order (NLO) or next-to-NLO based on the parton distribution functions. The background contribution from QCD multijet production where jets are misidentified as leptons is estimated from the data itself by using like-sign μ and τ_{had} events which were selected by inverting lepton identification and calorimeter isolation criteria. The samples are normalized to the data as function of p_T^{μ} and p_T^{τ} at an early stage of the selection in a region of phase space dominated by multijet production.

The $Z/\gamma \to ll$ cross section is calculated with CTEQ6L1 PDFs as $\sigma(Z/\gamma \to ll) = \sigma_{LO} \times K_{QCD}(Q^2)$, with the LO cross section calculated by Pythia LO PDF and the K_{QCD} at NNLO with NLO PDF, calculated according to [6, 7]. The $W \to \mu\nu$ is calculated with NNLO corrections and PDFs. The $t\bar{t}$ cross section is calculated at NNLO in [8] and the WW, ZZ and WZ cross sections are calculated with MCFM v3.4.5 CTEQ5L for LO and CTEQ5M (for NLO. The uncertainties due to the PDF uncertainty is calculated in [7].

III. EVENT SELECTION

Muons are selected using tracks in the central tracking detector in combination with patterns of hits in the muon detector. Muons are required to be isolated in both the calorimeter and the tracker.
A hadronically decaying tau lepton is characterized by a narrow isolated jet with low track multiplicity. The tau reconstruction is either seeded by calorimeter energy clusters or tracks. Three tau types are distinguished.

- τ-type I: a single track with a calorimeter cluster without any electromagnetic subclusters (1-prong, π-like).
- τ-type II: a single track with a calorimeter cluster and electromagnetic subclusters (1-prong, ρ-like).
- τ-type III: two or three tracks with an invariant mass below 1.1 or 1.7 GeV, respectively (3-prong).

A set of neural networks, one for each τ-type, is developed based on further discriminating variables. These input variables exploit the differences between hadronically decaying tau leptons and jets in the longitudinal and transverse shower shape as well as differences in the isolation in the calorimeter or in the tracker. The training of the neural network is performed using multijet events from data as the background sample and tau MC events as signal, resulting in a network output close to one for a tau candidate and close to zero for background. For τ-types I and II hadronic tau

candidates are required to have neural network output greater than 0.9. Due to the large background contamination τ-type III is neglected in the analysis at hand. The selection procedure is summarized briefly in Table I. The selection criteria have been adapted for the various Higgs boson masses in order to maximize the signal-to-background ratio. The selection will be justified and described more detailed in the following.

Selection criteria	$m_{\mathrm{H}} = 120$	$m_{\mathrm{H}} = 140$	$m_{\mathrm{H}} = 160$	$m_{\mathrm{H}} = 180$
Cut 1 Preselection	leptons from primary vertex large tau NN at least one SMT hit for the muon μ and τ not matched with $\Delta R(\eta, \phi) > 0.15$			
Cut 2 Missing Transverse Energy $\not\!\!E_{\mathrm{T}}$	> 20	> 20	> 20	> 20
Cut 3 $\not\!\!E_T^{\mathrm{Scaled}}$	> 7	> 7	> 7	> 7
Cut 4 $M_{min}^T\ (l, \not\!\!E_{\mathrm{T}})$	> 35	> 40	> 45	> 45
Cut 5 Sum of $p_T^l + p_T^{l'} + \not\!\!E_{\mathrm{T}}$	50-140	60-150	70-160	80-180
Cut 6 Invariant mass $M_{\mu\tau}$	< 50	< 60	< 60	< 80
Cut 7 H_T	< 70	< 70	< 70	< 70
Cut 8 $\Delta\phi(\mu, \tau)$	< 2	< 2	< 2	< 2

TABLE I: Summary of the selection criteria for the various Higgs boson masses $m_{\mathrm{H}} = 120$ GeV, $m_{\mathrm{H}} = 140$ GeV, $m_{\mathrm{H}} = 160$ GeV and $m_{\mathrm{H}} = 180$ GeV .

The selection requires two leptons with $p_T^\tau > 10$ GeV and $p_T^\mu > 12$ GeV, high τ NN output and originating from the primary vertex. They are required to match in η and ϕ with a reconstructed track. To reduce the background from photon conversions, at least one hit in the silicon tracking detector (SMT) is required for the muon. For suppressing background from muons, events are rejected in which the tau candidate can be matched to the muon. The signal is characterized by two leptons, missing transverse momentum and little jet activity. Figure 1a shows the invariant dilepton mass distribution in data, background and signal at this stage of the selection. This stage is referred to as preselection stage. Most of the QCD background is rejected by a selection requirement on the missing transverse Energy $\not\!\!E_{\mathrm{T}}$ and the scaled missing transverse energy $\not\!\!E_T^{\mathrm{Scaled}}$, which is the $\not\!\!E_{\mathrm{T}}$ divided by the $\not\!\!E_{\mathrm{T}}$ resolution. This quantity is particularly sensitive to events where the missing energy could be a result of mismeasurements of jet energies in the transverse plane. A selection requirement on the minimal transverse mass between one of the leptons and $\not\!\!E_{\mathrm{T}}$ reduces further the various background processes. Most of the $\mathrm{Z}/\gamma^* \to \ell\ell$ events are rejected by requiring the sum of the momentum of $p_T^\mu + p_T^\tau + \not\!\!E_{\mathrm{T}}$ to be more then 70 GeV and less than 160 GeV and to ask for the invariant dilepton mass to be less than $M_{\ell\ell} < 60$ GeV. The $\mathrm{t\bar{t}}$ contribution is reduced by requiring H_T to be lower than 70 GeV. H_T is defined as the scalar sum of the transverse momenta of all jets in the event. A large fraction of remaining back-to-back $\mathrm{Z}/\gamma^* \to \ell\ell$ is reduced by requiring an opening angle between the leptons of less than 2.0.

The selected signal contains two major contributions. $H \to WW \to \mu\tau_{had}$ events as well as $H \to WW \to e\mu$ final states were the electron is misreconstructed as tau. This will be indicated by the notation $H \to WW \to e_\tau\tau_{had}$ in the following. Generally the electronic events resemble the $WW \to \ell\ell$ background whereas the shape of the distributions of hadronic events is closer to $W + jet/\gamma$ background.

- $H \to WW \to e_\tau\mu$: (referred to as 'inclusive' sample in the following)
- $H \to WW \to \mu\tau_{had}$: (referred as 'exclusive' sample in the following)

After applying cuts 1-8 the remaining background is dominated by electroweak $W + jets/\gamma$ production. Further background reduction can not be easily achieved by cutting on one dimensional distributions. Therefore a likelihood approach has been used by constructing two likelihoods sensitive to different event properties. One likelihood is constructed using input distributions associated to the selected tau and will be referred to in the following as 'τ Likelihood'. The second one is based on kinematical properties of the particular event and will be referred as 'Kinematic Likelihood'. Both likelihoods are separately constructed according to formula (1), using either $H \to WW \to \mu\tau_{had}$ or $H \to WW \to e_\tau\mu$ events:

$$\mathcal{L} = \frac{\mathcal{P}_{Sig}(x_1, x_2, \ldots)}{\mathcal{P}_{Sig}(x_1, x_2, \ldots) + \mathcal{P}_{Bkgd}(x_1, x_2, \ldots} \approx \frac{\prod_i \mathcal{P}^i_{Sig}}{\prod_i \mathcal{P}^i_{Sig} + \prod_i \mathcal{P}^i_{Bkgd}} = \frac{\prod_i \mathcal{P}^i_{Sig}/\mathcal{P}^i_{Bkgd}}{\prod_i \mathcal{P}^i_{Sig}/\mathcal{P}^i_{Bkgd} + 1} \tag{1}$$

Whereas $\mathcal{P}^i_{Sig}$ represents the signal and $\mathcal{P}^i_{Bkgd}$ the background value for a given bin i. The value of the input distributions for bin i are given by the variables x_i. $\mathcal{P}^i_{Sig} \equiv \mathcal{P}_{Sig}(x_i)$ and $\mathcal{P}^i_{Sig} \equiv \mathcal{P}_{Sig}(x_i)$ represents the probability

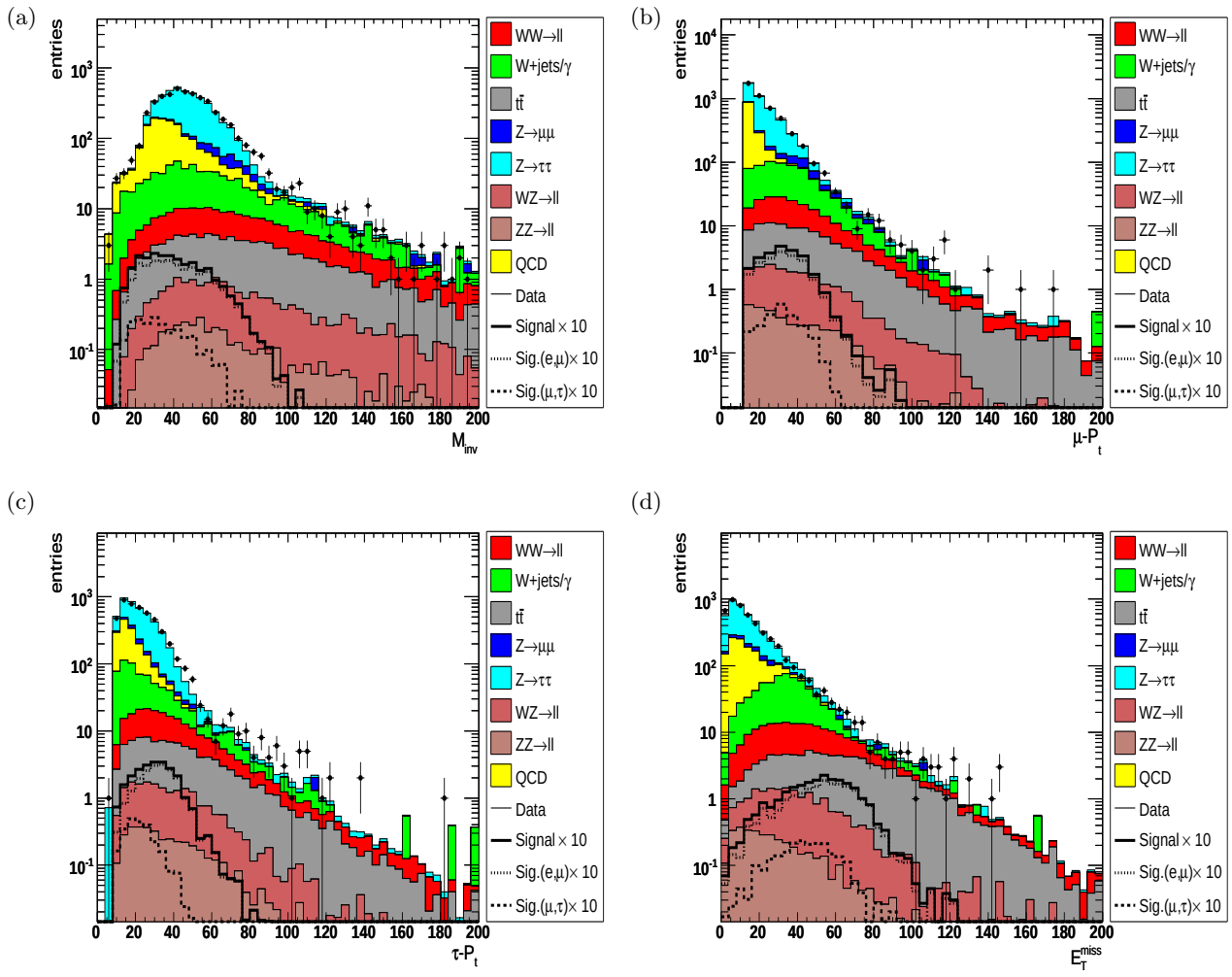

FIG. 1: Distribution of (a) the invariant dilepton mass at preselection level (b) the μ p_T at preselection level (b) the τ p_T at preselection level (d) the missing transverse energy, $\not\!\!E_{\rm T}$, at preselection level for data (points with error bars), background simulation (histograms, complemented with the QCD expectation) and signal expectation for $m_H = 160$ GeV (empty histogram). The various signal contributions $H \to WW \to e_\tau \mu$ and $H \to WW \to \mu \tau_h ad$ are given by dashed histograms.

density functions for the topological variables. For the construction of the τ likelihood the following variables are used:

- **EMF**: Fraction of the calorimeter energy deposited in the EM subcluster.
- $p_T^\tau + p_T^{trk}$: Sum of the transverse momenta of the track assigned to the tau and the energy deposited in the calorimeter
- τ **ID NN**: Output of the Neural Network
- E_T/p_T Ratio of Energy of calorimeter cluster and p_T of the leading track
- $\sum p_T^{trk}(\Delta \mathrm{R}(\tau, \mathrm{trk}) < 0.4)$: Sum p_T of all tracks in a Cone of 0.4 around the tau.

The second likelihood is based on kinematic quantities of the event:

- p_T^μ: p_T of the muon
- $M_T(\mu, \not\!\!E_{\rm T})$ Transverse mass of μ and $\not\!\!E_{\rm T}$
- $M_T^{min}(\ell, \not\!\!E_{\rm T})$ Minimal transverse mass of one lepton and $\not\!\!E_{\rm T}$
- $M_c = \sqrt{p_T^2(\ell\ell) + m^2(\ell\ell)} + \not\!\!E_{\rm T}$: cluster mass, approximation for the W mass.

training sample	τ-type	$m_{\mathrm{H}} = 120$	$m_{\mathrm{H}} = 140$	$m_{\mathrm{H}} = 160$	$m_{\mathrm{H}} = 180$
incl	I	$0.4 < \mathcal{L}_\tau < 0.8$	$\mathcal{L}_{kin} > 09$	$\mathcal{L}_{kin} > 0.9$ and $\mathcal{L}_\tau < 0.7$	$\mathcal{L}_{kin} > 0.9$ $\mathcal{L}_\tau > 0.8$
incl	II	$\mathcal{L}_\tau < 0.85$	$\mathcal{L}_\tau > 0.9$	$\mathcal{L}_{kin} > -\mathcal{L}_\tau + 1.3$	$\mathcal{L}_{kin} > 0.9$
excl.	I	$\mathcal{L}_\tau < 0.65$	$0.3 < \mathcal{L}_\tau < 0.85$ and $\mathcal{L}_{kin} < 0.1$	$\mathcal{L}_{kin} > 0.9$	$\mathcal{L}_{kin} > 0.9$
excl	II	$0.65 < \mathcal{L}_\tau < 0.8$	$0.6 < \mathcal{L}_\tau < 0.8$ and $\mathcal{L}_{kin} < 0.8$	$\mathcal{L}_{kin} > 0.9$	$\mathcal{L}_{kin} > 0.9$

TABLE II: List of the cuts applied on the 2D likelihood planes for both likelihood training classes and both selections.

- $\Delta\phi(\mu, \tau)$: Angle between μ and τ in the transverse plane.
- $\Delta\Theta(\mu, \tau)$: Solid angle between μ and τ

These likelihoods are constructed for each Higgs boson mass point. The resulting likelihood planes for $m_{\mathrm{H}} = 160$ GeV are displayed in Fig. 2. As last selection requirement a cut on this likelihood plane is applied. This selections have been optimized for each sample, tau type and Higgs Mass and are listed in Table. II.

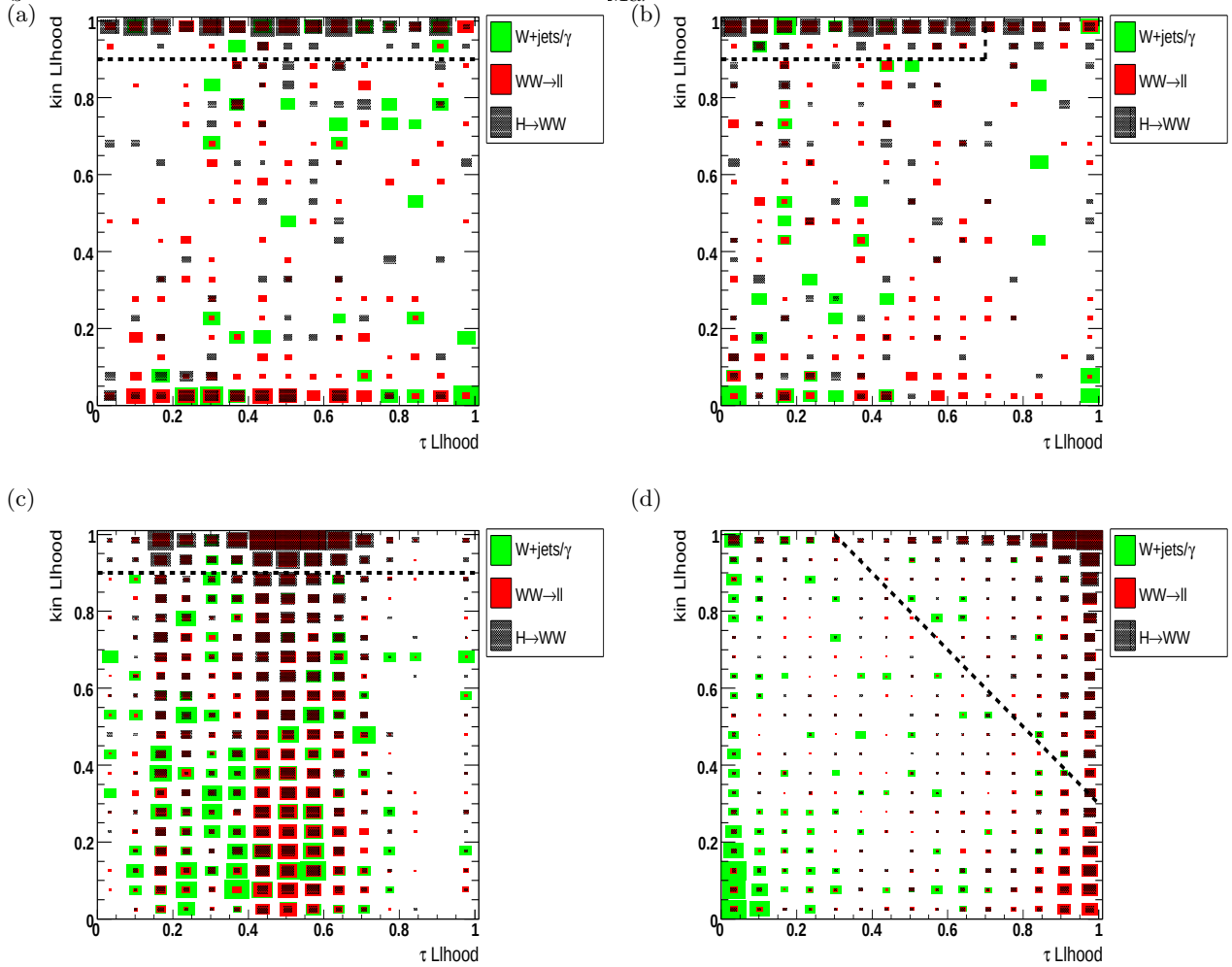

FIG. 2: 2 dimensional likelihood ouput for (a) τ-type I, and (c) τ-type II $H \to WW \to \mu\tau_h ad$ events. (b) (τ-type I) and (d) (τ-type II) show the output for selected $H \to WW \to e_\tau\mu$ events after cut 8. $W + jets/\gamma$ is given by the green histogram whereas red histograms represent $WW \to \ell\ell$ background. The black shaded area gives the selected signal in the corresponding final state. The black lines indicate the cuts applied to the selected signal. The signal MC used in this figure is generated with an Higgs boson mass of $m_{\mathrm{H}} = 160$ GeV.

In order to stay orthogonal to the corresponding $H \to WW^* \to e_\tau\mu$ analysis a veto on these events is applied after all selection requirements. This veto is as well applied for the construction of the likelihoods.

TABLE III: Number of candidate events observed and background events expected at different stages of the selection for τ type I, $m_{\rm H} = 120$ GeV and $m_{\rm H} = 140$ GeV. Errors are statistical only

	$m_{\rm H} = 120$ GeV			$m_{\rm H} = 140$ GeV		
Cut	Data	Tot. Exp. Bkgd	$H \to WW$	Data	Tot. Exp. Bkgd	$H \to WW$
Preselection	1749.00 ± 41.82	1719.19 ± 33.58	0.05	1749.00 ± 41.82	1719.19 ± 33.58	0.15
$\Delta\phi(\mu,\tau)$	47.00 ± 6.86	42.36 ± 3.96	0.02	39.00 ± 6.24	38.60 ± 3.81	0.07
Final Sel. incl.	19.00 ± 4.36	20.36 ± 2.71	0.02	3.00 ± 1.73	7.36 ± 1.57	0.02
Final Sel. excl.	17.00 ± 4.12	12.04 ± 2.31	0.00	6.00 ± 2.45	4.94 ± 1.36	0.01

TABLE IV: Number of candidate events observed and background events expected at different stages of the selection for τ type I, $m_{\rm H} = 160$ GeV and $m_{\rm H} = 180$ GeV. Errors are statistical only

	$m_{\rm H} = 160$ GeV			$m_{\rm H} = 180$ GeV		
Cut	Data	Tot. Exp. Bkgd	$H \to WW$	Data	Tot. Exp. Bkgd	$H \to WW$
Preselection	1749.00 ± 41.82	1719.19 ± 33.58	0.20	1749.00 ± 41.82	1719.19 ± 33.58	0.15
$\Delta\phi(\mu,\tau)$	30.00 ± 5.48	21.66 ± 2.74	0.11	31.00 ± 5.57	24.26 ± 2.87	0.07
Final Sel. incl.	2.00 ± 1.41	4.63 ± 1.22	0.05	1.00 ± 1.00	1.25 ± 0.60	0.01
Final Sel. excl.	3.00 ± 1.73	1.78 ± 0.68	0.01	3.00 ± 1.73	5.79 ± 1.27	0.03

IV. SYSTEMATIC UNCERTAINTIES

The following sources of systematic uncertainties on the number of background and expected signal events were taken into account: Lepton identification and reconstruction efficiencies (0.3–3.6%), jet energy scale calibration in signal and background events($< 2\%$), track momentum calibration (4%), detector modeling (1% for signal, 5-10% for background), PDF uncertainties (4%), and modeling of multijet background (5%). The systematic error on the luminosity on the normalization of the cross section is conservatively taken to be 10%, resulting from the NNLO $Z/\gamma \to \ell\ell$ cross section uncertainty (3.6%), the uncertainty on the QCD background (5%) and the uncertainty on the Z peak mass window (6%) added in quadrature. The uncertainty to the modeling of the electroweak $W + jet/\gamma$ production has been estimated to be 2.5-17.5%. In total the systematic error varies between 8.7–20.9% for background and 8.9–10.1% for Signal. However, the systematic error is small compared to the statistical error.

V. RESULTS

Numbers of observed candidates and background events expected after application of the successive selections for $m_{\rm H} = 120, 140, 160$ and 180 GeV are listed in Tab. III, IV for τ-type I and in Tab. V, VI for τ-type II events. Since after all selection cuts the remaining candidate events are consistent with a background observation, limits on the production cross section times branching ratio $\sigma \times BR(H \to WW^*)$ are derived following the method described in Ref. [9].

The total background expectation is dominated by $W + jets/\gamma$ and di-boson events. The number of signal events are in the range of 0.0-0.41 events in the final selection.

TABLE V: Number of candidate events observed and background events expected at different stages of the selection for τ type II, $m_{\mathrm{H}} = 120$ GeV and $m_{\mathrm{H}} = 140$ GeV. Errors are statistical only

	$m_{\mathrm{H}} = 120$ GeV			$m_{\mathrm{H}} = 140$ GeV		
Cut	Data	Tot. Exp. Bkgd	$H \to WW$	Data	Tot. Exp. Bkgd	$H \to WW$
Preselection	4786.00 ± 69.18	4737.06 ± 47.96	0.65	4786.00 ± 69.18	4737.06 ± 47.96	1.96
$\Delta\phi(\mu,\tau)$	143.00 ± 11.96	140.17 ± 6.36	0.35	124.00 ± 11.14	133.15 ± 5.99	1.03
Final Sel incl.	42.00 ± 6.48	42.35 ± 3.47	0.14	25.00 ± 5.00	28.82 ± 2.77	0.29
Final Sel. excl.	21.00 ± 4.58	29.19 ± 3.06	0.01	27.00 ± 5.20	39.97 ± 3.47	0.07

TABLE VI: Number of candidate events observed and background events expected at different stages of the selection for τ type II, $m_{\mathrm{H}} = 160$ GeV and $m_{\mathrm{H}} = 180$ GeV. Errors are statistical only

	$m_{\mathrm{H}} = 160$ GeV			$m_{\mathrm{H}} = 180$ GeV		
Cut	Data	Tot. Exp. Bkgd	$H \to WW$	Data	Tot. Exp. Bkgd	$H \to WW$
Preselection	4786.00 ± 69.18	4735.08 ± 47.95	2.47	4786.00 ± 69.18	4737.06 ± 47.96	1.87
$\Delta\phi(\mu,\tau)$	98.00 ± 9.90	101.90 ± 5.05	1.42	108.00 ± 10.39	111.55 ± 5.08	1.04
Final Sel incl.	15.00 ± 3.87	14.11 ± 1.76	0.27	21.00 ± 4.58	14.12 ± 1.69	0.18
Final Sel excl.	8.00 ± 2.83	7.08 ± 1.37	0.05	2.00 ± 1.41	5.10 ± 1.10	0.01

Since no evidence for production of a Standard Modell Higgs boson is observed, upper limits on the product of cross section and leptonic branching fraction $H \to WW \to \mu + \tau_{had}$ and $H \to WW \to \mu + e$ can be set (Tab. VII).

A graphical representation of the expected and observed limits for the analyzed Higgs boson masses $m_{\mathrm{H}} = 120, 140, 160$ and 180 GeV is displayed in Fig. 3.

VI. CONCLUSIONS

A search has been performed for the $H \to WW \to \ell\ell$ decay signature from the associated production of the Standard Model Higgs boson in leptonic channels with muons and taus, using data corresponding to an integrated luminosity of 1000 pb^{-1} . No evidence for the Higgs particle is observed and the first upper limits using this channel on the product of cross section times branching ratio are set. Combined with existing $H \to WW \to \ell\ell$ analysis previous limits can be improved.

	$m_{\mathrm{H}} = 120$ GeV		$m_{\mathrm{H}} = 140$ GeV		$m_{\mathrm{H}} = 160$ GeV		$m_{\mathrm{H}} = 180$ GeV	
	expected	observed	expected	observed	expected	observed	expected	observed
τ-type I	90.2 pb	90.4 pb	68.7 pb	51.7 pb	28.2 pb	22.6 pb	29.4 pb	20.7 pb
τ-type II	14.8 pb	14.8 pb	13.6 pb	10.5 pb	9.9 pb	10.9 pb	10.3 pb	17.0 pb
comb.	15.1 pb	14.6 pb	13.2 pb	9.9 pb	9.2 pb	9.7 pb	9.7 pb	13.0 pb

TABLE VII: Final limit for the combination of all contributing channels and for $m_{\mathrm{H}} = 120, 140, 160, 180$ GeV

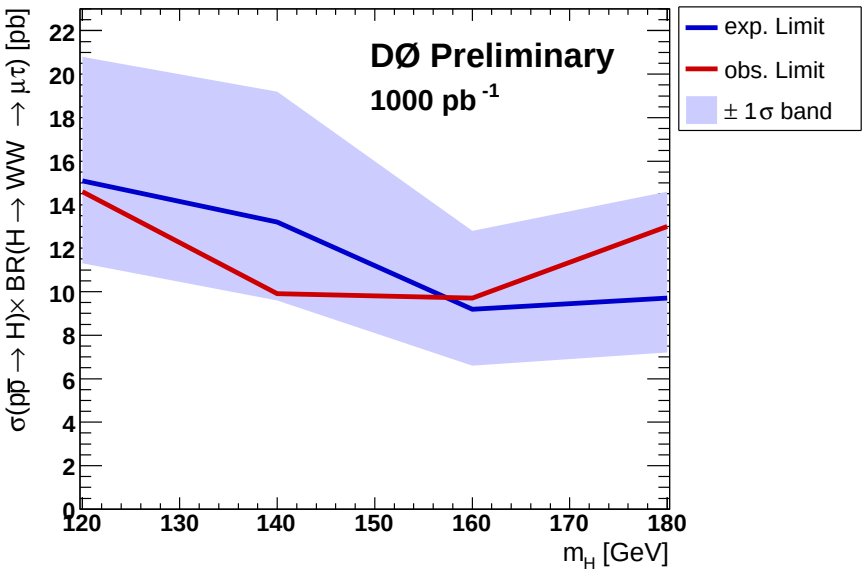

FIG. 3: Expected and observed limits for $m_{\rm H} = 120, 140, 160, 180$ GeV. The red line represents the observed limit and the blue one the expected limit. The error for the expected limit given by the shaded area corresponds to $\pm 1\sigma$ for a C.L. of 95%.

Acknowledgments

We thank the staffs at Fermilab and collaborating institutions, and acknowledge support from the Department of Energy and National Science Foundation (USA), Commissariat à l'Energie Atomique and CNRS/Institut National de Physique Nucléaire et de Physique des Particules (France), Ministry of Education and Science, Agency for Atomic Energy and RF President Grants Program (Russia), CAPES, CNPq, FAPERJ, FAPESP and FUNDUNESP (Brazil), Departments of Atomic Energy and Science and Technology (India), Colciencias (Colombia), CONACyT (Mexico), KRF (Korea), CONICET and UBACyT (Argentina), The Foundation for Fundamental Research on Matter (The Netherlands), PPARC (United Kingdom), Ministry of Education (Czech Republic), Natural Sciences and Engineering Research Council and WestGrid Project (Canada), BMBF (Germany), A.P. Sloan Foundation, Civilian Research and Development Foundation, Research Corporation, Texas Advanced Research Program, and the Alexander von Humboldt Foundation.

[1] T. Hao, A. Turcot, R-J. Yang, Phys. Rev. D. 59, 093001 (1999).
[2] M. Carena *et al.* [Higgs Working Group Collaboration], "Report of the Tevatron Higgs working group", hep-ph/0010338.
[3] K. Jakobs, W. Walkowiak, ATLAS Physics Note, ATL-PHYS-2000-019.
[4] M. Titov, D0 Note 005063, "Search for the Higgs boson in $H \to WW \to l^+l^-(ee, e\mu)$ decays with 950 pb^{-1} at DO in Run II"
[5] T. Sjöstrand, Comp. Phys. Commun. **82** (1994) 74, `CERN-TH 7112/93` (1993).
[6] R. Hamberg, W.L. van Neerven, and T. Matsuura, Nucl. Phys. **B359**, 343 (1991) [Erratum-ibid. **B644**, 403 (2002)].
[7] T. Nunnemann, D0 Note 4476.
[8] N. Kidonakis, R. Vogt, hep-ph/0410367, published in Int.J.Mod.Phys.A20:3171, 2005.
[9] T. Junk, Nucl. Instr. and Meth., A434(1999) 435